3. M. Cannat *et al.*, *Geology* **23**, 49 (1995).
4. The pressures both at room temperature and at high temperatures were estimated on the basis of the unit cell volume changes of Au with an equation of state [O. L. Anderson, D. G. Isaak, S. Yamamoto, *J. Appl. Phys.* **65**, 1534 (1989)].
5. There were significant temperature gradients across the sample charge, and the uncertainty of the temperature measurements may be on the order of ±50°C, though we tried to examine the sample that was very close (~0.1 mm) to the hot junction of the thermocouple.
6. The hybrid anvil system [T. Irifune, W. Utsumi, T. Yagi, *Proc. Jpn. Acad.* **68**, 161 (1992)] uses four tungsten carbide (WC) and four advanced diamond composite (ADC) anvils for the double-stage anvil (MA8) system. The assembled anvil cube was pressurized in cubic presses (MAX80 and MAX90) at KEK [O. Shimomura, W. Utsumi, T. Taniguchi, T. Kikegawa, T. Nagashima, in *High-Pressure Research: Application to Earth and Planetary Sciences*, Y. Syono and M. H. Manghnani, Eds. [Terra Scientific (TERRAPUB)/American Geophysical Union (AGU), Tokyo/Washington, DC, 1992), pp. 3–11]. A white x-ray beam from the synchrotron radiation was introduced from the anvil gap through vertical (300 μm) and horizontal (50 μm) slits and irradiated onto the sample near the hot junction of the thermocouple. The diffracted x-ray beam was collected through vertical (500 μm) and horizontal (50 μm) slits at the fixed positions of $2\theta = 4°$ and 6°. An energy dispersive method was adopted with a solid-state detector and a multichannel analyzer. One of the ADC anvils was used for the window to direct the diffracted x-ray beam, because this material is highly transparent to the x-ray of a wide range of photon energies.
7. While the temperature was increased to about 500°C, the pressure dropped significantly (Fig. 1), probably because the pyrophyllite gaskets yielded as a result of stress relaxation within the sample. At still higher temperatures, however, the pressure increased again and approached the initial value.
8. The x-ray diffraction peaks of the quenched sample, after subtracting a few peaks that correspond to superhydrous B, were consistent with those of phase D [L. Liu, *Phys. Earth Planet. Inter.* **49**, 142 (1987)]. The phases in the products from our runs, however, contained about 15 weight % H_2O as estimated from the deficit of the oxide total of the electron microprobe analysis and had a Si/Mg ratio of ~1.5, which is quite different from that proposed for phase D. This composition is rather close to that of phase F synthesized at pressures above 15 GPa [M. Kanzaki, *ibid.* **66**, 307 (1991)], but our x-ray diffraction pattern is completely different from those reported for phase F [Y. Kudoh, T. Nagase, S. Sasaki, M. Tanaka, M. Kanzaki, *Phys. Chem. Mineral.* **22**, 295 (1995)].
9. T. Wu, W. A. Bassett, P. C. Burnley, M. S. Weathers, *J. Geophys. Res.* **98**, 19767 (1993).
10. K. Fujino and T. Irifune, in *High-Pressure Research: Application to Earth and Planetary Sciences*, Y. Syono and M. H. Manghnani, Eds. (TERRAPUB/AGU, Tokyo/Washington, DC, 1992), pp. 237–243.
11. P. Ulmer and V. Trommsdorff, *Science* **268**, 858 (1995).
12. D. L. Turcotte and G. Schubert, *Geodynamics* (Wiley, New York, 1982); G. R. Helffrich, S. Stein, B. J. Wood, *J. Geophys. Res.* **94**, 753 (1989); S. H. Kirby *et al.*, *Science* **252**, 216 (1991).
13. P. G. Silver *et al.*, *Science* **268**, 69 (1995).
14. E. Ito and T. Katsura, *Geophys. Res. Lett.* **16**, 425 (1989).
15. We thank S. Urakawa, T. Ohtani, K. Fujino, T. Kikegawa, O. Shimomura, and M. Miyashita for their help and encouragement during the x-ray diffraction experiments at KEK. The antigorite specimen was provided by T. Minakawa. Supported by Grant-in-Aid for Scientific Research from the Ministry of Education, Science and Culture of the Japanese Government, and by the Japan Society for the Promotion of Science.

12 February 1996; accepted 18 April 1996

Blockage by Adenovirus E4orf6 of Transcriptional Activation by the p53 Tumor Suppressor

Thomas Dobner, Nobuo Horikoshi, Susanne Rubenwolf, Thomas Shenk*

The adenovirus E4orf6 protein is shown here to interact with the cellular tumor suppressor protein p53 and to block p53-mediated transcriptional activation. The adenovirus protein inhibited the ability of p53 to bind to human $TAF_{II}31$, a component of transcription factor IID (TFIID). Earlier work demonstrated that the interaction of p53 with $TAF_{II}31$ involves a sequence near the NH_2-terminus of p53, whereas the E4orf6-p53 interaction occurs within amino acids 318 to 360 of p53. Thus, the E4orf6 protein interacts at a site on p53 distinct from the domain that binds to $TAF_{II}31$ but nevertheless inhibits the p53-$TAF_{II}31$ interaction.

The transcriptional regulatory protein p53 (*1*) activates the expression of proteins that control cellular growth (*2*). Inhibition of its ability to activate transcription correlates with oncogenesis (*3*). Three functional domains of p53 have been defined (*4*): an NH_2-terminal transcriptional activation domain (amino acids 1 to 42), a central DNA binding domain (amino acids 120 to 290), and a COOH-terminal regulatory domain (amino acids 311 to 393). The DNA binding domain recognizes a DNA motif in genes that are activated by p53 (*5*). Mutations in p53 that arise in human cancers generally cluster in its DNA binding domain (*6*). The NH_2-terminal activation domain stimulates transcription by interacting with $TAF_{II}31$, a constituent of TFIID, in the transcriptional initiation complex (*7*). The MDM-2 oncoprotein (*8*) and the adenovirus E1B 55-kD oncoprotein (*9*) each bind to this domain of p53, blocking its activation function. The COOH-terminal domain of p53 contains an oligomerization domain as well as sequences that modulate DNA binding by p53. An antibody that binds within this domain stimulates sequence-specific DNA binding by p53 (*10*), as does phosphorylation within this domain (*10–13*). The COOH-terminal domain of p53 also can bind to single-stranded nucleic acids (*4*, *14*, *15*), and short single strands of DNA markedly stimulate sequence-specific DNA binding by the central domain of p53 (*15*). In this report, we demonstrate that the adenovirus E4orf6 protein binds to the COOH-terminal regulatory domain of p53. However, rather than modulate DNA binding, the viral protein inhibits the interaction of the NH_2-terminal activation domain with the transcriptional initiation complex.

The adenovirus E1B 55-kD protein can bind to both p53 (*9*) and the adenovirus E4orf6 protein (*16*), which raises the possibility that the three proteins might form a complex within adenovirus-infected cells. Therefore, we examined whether the E4orf6 protein can influence transcriptional activation by p53 (*17*). Initially, we assayed the effect of E4orf6 on the activity of a reporter gene containing two copies of the p53 binding site from the muscle creatine kinase gene in p53-deficient SAOS-2 cells (Fig. 1A). Cotransfection of a plasmid expressing p53 with the reporter enhanced expression by a factor of about 6, whereas inclusion of a third plasmid expressing the E4orf6 protein blocked the ability of p53 to enhance expression from the reporter. In control experiments (Fig. 1A), an E1B 55-kD protein expression plasmid blocked p53-mediated induction of the reporter as predicted (*9*); the expression cassette without an inserted E4orf6 complementary DNA (pDCR) had no effect on activation by p53, which rules out the possibility that the inhibition observed was the result of promoter competition.

The E4orf6 protein also blocked the induction of a reporter gene containing Gal4 DNA binding sites by a Gal4-p53 fusion protein within HeLa cells (Fig. 1B). The E4orf6 protein inhibited activation by Gal4-p53 in a dose-dependent fashion as efficiently as the E1B 55-kD protein did. The expression cassette without the E4orf6 insert (pDCR) did not influence expression from the reporter (Fig. 1B); expression of the Gal4 DNA binding domain with no fusion partner (pSG424) did not influence activity of the reporter (Fig. 1C). Although expression of

T. Dobner and S. Rubenwolf, Institut für Medizinische Mikrobiologie und Hygiene, Universität Regensburg, D-93042 Regensburg, Germany.
N. Horikoshi and T. Shenk, Howard Hughes Medical Institute, Department of Molecular Biology, Princeton University, Princeton, NJ 08544, USA.

*To whom correspondence should be addressed.

the E4orf6 protein inhibited activation by the Gal4 fusion protein containing the entire p53 coding region (pGalp53), it did not influence activation by a fusion protein with only the NH_2-terminal activation domain of p53 (pGalp53N) (Fig. 1C). A Gal4 fusion protein containing the COOH-terminal region of p53 can repress expresssion from a reporter with Gal4 DNA binding sites (*18*); E4orf6 protein relieved the repression in a dose-dependent manner, whereas the unrelated E4orf3 protein had no effect (Fig. 1C). Thus, the E4orf6 protein influenced the activity of Gal4 fusion proteins containing the COOH-terminal region of p53, whereas it did not influence the activity of a fusion construct including only the NH_2-terminal activation domain of p53, which suggests that the E4orf6 protein targets the COOH-terminal region of p53.

The E1B 55-kD protein represses transcription when brought to DNA through a Gal4 DNA binding domain (*19*). In contrast to the E1B 55-kD protein, the E4orf6 protein displayed little intrinsic repression activity when tethered to DNA (Fig. 1D).

To test the ability of the E4orf6 protein to interact with p53 and to map the site of the possible interaction on p53, we performed a protein blot (*20*). Glutathione-S-transferase (GST) fusion proteins containing segments of p53 were subjected to electrophoresis and transferred to a membrane (Fig. 2B). The bound proteins were then reacted with E4orf6 or E1B 55-kD protein plus antibodies to the viral proteins. As shown previously (9), the E1B 55-kD protein interacted with an NH_2-terminal but not a COOH-terminal segment of p53 (Fig. 2B). In contrast, the E4orf6 protein did not interact with the NH_2-terminal domain; rather, it reacted with fusion proteins that included the COOH-terminal region of p53 (Fig. 2B). The site of E4orf6 protein interaction on p53 was confirmed and refined with the use of GST fusion proteins containing segments of p53 to capture in vitro–translated E4orf6 protein (Fig. 2C). Fusion proteins containing p53 amino acids 318 to 360 or 318 to 393 interacted with the E4orf6 protein, whereas only background binding was evident when a fusion protein containing p53 amino acids 360 to 393 was tested. The E4orf6 protein interacted within amino acids 318 to 360 of p53 (Fig. 2A).

To determine whether a p53-E4orf6 interaction occurs within infected cells, a p53-specific antibody was used to immunoprecipitate p53 and its associated proteins, which we then assayed by protein immunoblot using an E4orf6-specific antibody (*21*). More p53 was immunoprecipitated from cells infected with the two mutant viruses, in which larger amounts of p53 accumulated than in cells infected with the wild-type virus (*22*). The E4orf6 protein was co-immunoprecipitated with p53 from cells infected with wild-type adenovirus (*wt*300, where the number indicates the virus number) but not from cells infected with a mutant virus (*dl*355) lacking E4orf6 (Fig. 3A). The p53-E4orf6 interaction was also evident in cells infected with a virus (*dl*338) lacking the gene encoding 55-kD E1B, which demonstrates that its product (which interacts with both p53 and E4orf6 proteins) is not needed for the in vivo p53-E4orf6 interaction. The E4orf6-specific antibody also recognizes the E4orf6/7 protein because the two proteins share 58 amino acids at their NH_2-termini, and the E4orf6/7 protein was co-immunoprecipitated with p53 (Fig. 3A). The p53-E4orf6/7 interaction is probably indirect because in vitro–translated E4orf6/7 protein was captured very inefficiently by GST-p53 fusion proteins (Fig. 3B). Further, in contrast to the E4orf6 protein, the E4orf6/7 protein did not inhibit the activation of transcription by p53 (Fig. 3C).

Earlier work showing that the COOH-terminal domain of p53 regulates the activity of its central DNA binding domain (*10–15*) led us to suspect that the interaction of the E4orf6 protein within the COOH-terminal region of p53 might interfere with the ability of p53 to bind to DNA. However, p53 bound equally well to its recognition site in the presence or absence of E4orf6 protein (*23*). Because p53 interacts with both DNA and $TAF_{II}31$ (a constituent of TFIID) to activate transcription (*4*, *7*), we examined whether the E4orf6 protein influenced the p53-$TAF_{II}31$ interaction (*24*). We mixed p53 alone or in the presence of E4orf6 protein with an excess of GST-$TAF_{II}31$ fusion protein, and the captured proteins were detected by protein immunoblot assay with the use of antibodies to the p53 and E4orf6 proteins. Approximately 8% of the input p53 was bound by the fusion protein in the absence of E4orf6

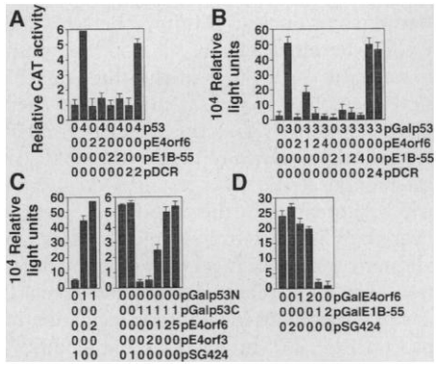

Fig. 1. The E4orf6 protein inhibits transcriptional control by p53. (**A**) CAT assays in SAOS-2 cells, showing that E4orf6 (pE4orf6) and 55-kD E1B (pE1B-55), but not the expression vector (pDCR), block activation of a reporter (p50-2) by p53. (**B**) Luciferase assays in HeLa cells, showing that E4orf 6 blocks activation of a reporter (pGalTK-LUC) by a fusion protein containing the complete p53 sequence (pGalp53). (**C**) Luciferase assays in H1299 cells demonstrating that E4orf6 blocks repression of a reporter by a Gal4 fusion protein containing p53 amino acids 80 to 393 (pGalp53C), but not by a fusion protein containing p53 amino acids 1 to 52 (pGal4p53N). pSG424 encodes the Gal4 DNA binding domain with no fusion partner. (**D**) Luciferase assays in HeLa cells, showing that a Gal4 fusion protein containing the E1B 55-kD protein (pGalE1B-55) represses, whereas a Gal4-E4orf6 fusion protein (pGalE4orf6) does not significantly influence expression of a reporter. All transfections received 3 μg of reporter plasmid per 3×10^5 cells plus the quantity of effector plasmid (micrograms of DNA per 3×10^5 cells) tabulated below each bar in the graphs. The average and standard deviation is presented for two experiments, each performed in duplicate.

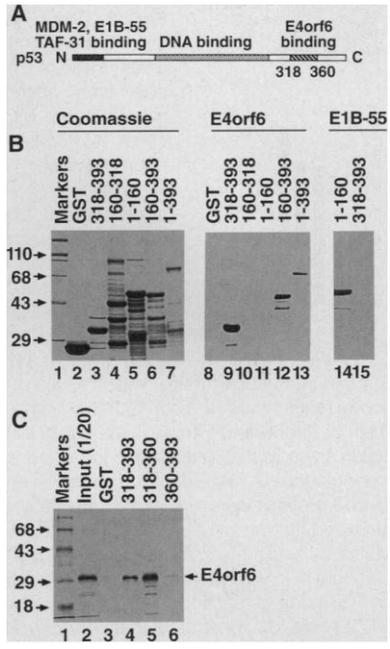

Fig. 2. The E4orf6 protein interacts within a 43–amino acid domain near the COOH-terminus of p53. (**A**) Diagram of p53 showing the E4orf6 binding domain relative to major landmarks. Amino acids bracketing the E4orf6 binding domain are identified. (**B**) Protein blot experiment. GST-p53 fusion proteins were subjected to electrophoresis and transferred to nitrocellulose (the range of p53 amino acids present in fusion proteins is indicated above the lanes). The bound proteins were then assayed by Coomassie blue staining (lanes 1 to 7) or by incubation with purified E4orf6 (lanes 8 to 13) or with 55-kD E1B (lanes 14 and 15) followed by reaction with antibodies specific to the viral proteins. (**C**) GST capture experiment. GST-p53 fusion proteins were assayed for their ability to bind E4orf6. Lane 2, input, received 1/20 of the amount of E4orf6 added to each GST capture reaction. Autoradiograms were scanned and cropped with Photoshop, and figures were prepared with FreeHand software.

protein (Fig. 4). When increasing amounts of E4orf6 protein were mixed with the p53 before the addition of the fusion protein, the p53-$TAF_{II}31$ interaction was progressively inhibited (Fig. 4). A fivefold molar excess of E4orf6 protein relative to p53 reduced the amount of p53 captured by the GST-$TAF_{II}31$ protein by a factor of about 6. No E4orf6 protein was captured together with the p53 (Fig. 4), which indicates that the p53-E4orf6 and p53-$TAF_{II}31$ interactions are mutually exclusive.

Our results demonstrate that the adenovirus E4orf6 protein can interact with p53 both in vitro and within virus-infected cells (Figs. 2 and 4) and block its ability to activate expression of p53-responsive promoters (Fig. 1). The p53-E4orf6 interaction occurs within amino acids 318 to 360 of p53 (Fig. 2). This region is also responsible for p53 tetramerization (*25*), and it lies within the COOH-terminal region that regulates DNA binding by the tumor suppressor protein (*10–15*). However, E4orf6 protein does not influence the ability of p53 to oligomerize or to bind to DNA (*23*). Rather, it interferes with the interaction of p53 and $TAF_{II}31$ (Fig. 4), an interaction that presumably allows DNA-bound p53 to communicate with the initiation complex and to stimulate transcription (*7*). Inhibition of the p53-$TAF_{II}31$ interaction is consistent with the ability of E4orf6 protein to block transcriptional activation by a Gal4-p53 fusion protein (Fig. 1) where DNA binding is mediated by Gal4 sequences.

The E4orf6 protein is the first example of a protein that binds within the COOH-terminal region of p53 and regulates the contact of the NH_2-terminal domain of p53 with $TAF_{II}31$. The mechanism by which E4orf6 binding abrogates the p53-$TAF_{II}31$ interaction remains unclear. Possibly, the NH_2 and COOH-terminal regions of p53 are positioned near each other in the three-dimensional structure of p53. If this is true, then E4orf6 binding within the COOH-terminal region might sterically hinder the $TAF_{II}31$ interaction at the NH_2-terminal domain of p53. Alternatively, the E4orf6 interaction near the COOH-terminus might induce an allosteric transition in p53, altering the function of its NH_2-terminal activation domain. There is precedent for allosteric regulation in p53 (*10*, *11*, *26*). Interactions and modifications within the COOH-terminal regulatory domain can modulate DNA binding by p53.

Because the adenovirus E1B 55-kD and E4orf6 proteins bind to different domains on p53, they might bind to p53 simultaneously and cooperate to antagonize p53 function. p53 might also contribute to the function of the E1B 55-kD–E4orf6 complex (*16*) that regulates mRNA transport in virus-infected cells (*27*). Most adenovirus vectors being considered for human gene therapy applications contain the E4orf6 coding region. It would be prudent to remove this gene from vectors, given the protein's ability to antagonize a function of p53 that correlates with its tumor suppressor activity.

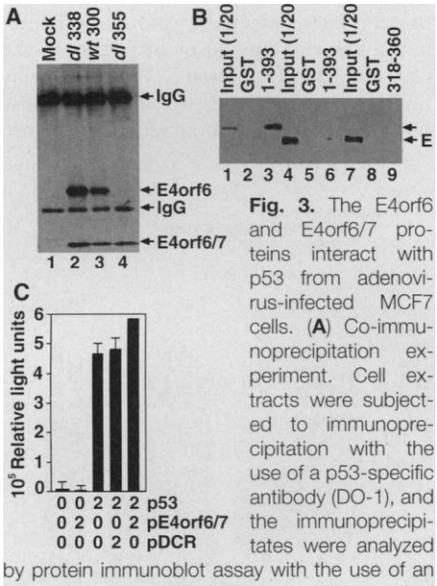

Fig. 3. The E4orf6 and E4orf6/7 proteins interact with p53 from adenovirus-infected MCF7 cells. (**A**) Co-immunoprecipitation experiment. Cell extracts were subjected to immunoprecipitation with the use of a p53-specific antibody (DO-1), and the immunoprecipitates were analyzed by protein immunoblot assay with the use of an antibody reacting with the common NH_2-terminal domain of E4orf6 and E4orf6/7. Viruses used for infection are indicated at the top of the lanes. IgG, immunoglobulin G. (**B**) GST capture experiment. GST-p53 proteins were assayed for their ability to bind E4orf6 (top arrow) and E4orf6/7 (bottom arrow). Lanes designated "input" received 1/20 of the amount of in vitro–translated protein added to each GST capture reaction. (**C**) Luciferase assays in H1299 cells, demonstrating that E4orf6/7 does not inhibit p53-mediated transcriptional activation of a reporter (pRELUC). pDR is the expression vector with no inserted effector gene. The average and standard deviation are presented for two experiments, each performed in duplicate.

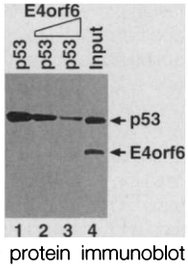

Fig. 4. The E4orf6 protein blocks the interaction of p53 with $TAF_{II}31$. We incubated p53 alone (lane 1) or a 1:1 mixture (lane 2) or a 1:5 mixture (lane 3) of p53 and E4orf6 with GST-$TAF_{II}31$. Complexes were captured on glutathione-Sepharose beads, and proteins were detected by protein immunoblot with the use of a mixture of antibodies to p53 (mAb 421) and E4orf6 (RSA3). Lane 4, input, received a 1:5 p53-E4orf6 mixture (1/20 the amount added to capture reactions).

REFERENCES AND NOTES

1. S. Fields and S. K. Jang, *Science* **249**, 1046 (1990); R. W. O'Rourke *et al.*, *Oncogene* **5**, 1829 (1990); L. Raycroft, H. Wu, G. Lozano, *Science* **249**, 1049 (1990).
2. W. S. El-Deiry *et al.*, *Cell* **75**, 817 (1993).
3. Reviewed in G. P. Zambetti and A. J. Levine, *FASEB J.* **7**, 855 (1993).
4. C. Prives *et al.*, *Cold Spring Harbor Symp. Quant. Biol.* **59**, 207 (1994).
5. Reviewed in B. Vogelstein and K. W. Kinzler, *Cell* **70**, 523 (1992).
6. A. J. Levine *et al.*, *J. Lab. Clin. Med.* **124**, 817 (1994).
7. H. Lu and A. J. Levine, *Proc. Natl. Acad. Sci. U.S.A.* **92**, 5154 (1995); C. J. Thut, J.-L. Chen, R. Klemm, R. Tjian, *Science* **267**, 100 (1995).
8. J. Momand, G. P. Zambetti, D. C. Olson, D. George, A. J. Levine, *Cell* **69**, 1237 (1992); J. Chen, V. Marechal, A. J. Levine, *Mol. Cell. Biol.* **13**, 4107 (1993); J. D. Oliner *et al.*, *Nature* **362**, 857 (1993).
9. P. Sarnow, Y. S. Ho, J. Williams, A. J. Levine, *Cell* **28**, 387 (1982); C. C. Kao, P. R. Yew, A. J. Berk, *Virology* **52**, 456 (1990); P. R. Yew and A. J. Berk, *Nature* **357**, 82 (1992).
10. T. R. Hupp, D. W. Meek, C. A. Midgley, D. P. Lane, *Cell* **71**, 875 (1992).
11. T. R. Hupp and D. P. Lane, *Curr. Biol.* **4**, 865 (1994).
12. Y. Wang and C. Prives, *Nature* **376**, 88 (1995).
13. I. Takenaka, F. Morin, B. R. Seizinger, N. Kley, *J. Biol. Chem.* **270**, 5405 (1995).
14. R. Brain and J. R. Jenkins, *Oncogene* **9**, 1775 (1994); L. Wu, H. Bayle, B. Elenbaas, N. P. Pavletich, A. J. Levine, *Mol. Cell. Biol.* **15**, 497 (1995).
15. J. Jayaraman and C. Prives, *Cell* **81**, 1021 (1995).
16. P. Sarnow *et al.*, *J. Virol.* **49**, 692 (1984).
17. SAOS-2, HeLa, or H1299 cells were transfected with 3 μg of a reporter plasmid, p50-2CAT [G. P. Zambetti, J. Bargonetti, K. Walker, C. Prives, A. J. Levine, *Genes Dev.* **6**, 1143 (1992)] or pGalTK-LUC, which contains five Gal4 DNA binding sites upstream of the herpes virus thymidine kinase promoter that controls expression of luciferase, plus various amounts of effector plasmids. Effector plasmids used the cytomegalovirus major immediate early promoter to express p53 (p53); Gal4-p53 fusion proteins, p53 amino acids 1 to 393 (pGalp53), 1 to 52 (pGalp53N), or 80 to 393 (pGalp53C); adenovirus proteins, 55-kD E1B (pE1B-55), E4orf3 (pE4orf3), or E4orf6 (pE4orf6); or Gal4 fusion proteins containing adenovirus 55-kD E1B (pGalE1B-55) or E4orf6 (pGalE4orf6). Cells were harvested 48 hours (luciferase assays) or 72 hours (chloramphenicol acetyltransferase assays) after transfection, and enzyme activities were quantified.
18. N. Horikoshi *et al.*, *Mol. Cell. Biol.* **15**, 227 (1995).
19. P. R. Yew, X. Liu, A. J. Berk, *Genes Dev.* **8**, 190 (1994).
20. GST fusion proteins containing segments of p53 (*18*) were purified by binding to glutathione-Sepharose, subjected to electorphoresis, and transferred to a nitrocellulose membrane. Protein bound to the nitrocellulose was monitored with the use of Coomassie blue strain. To test for protein interactions, histidine-tagged 55-kD E1B and E4orf6 from baculovirus-infected cells were incubated with the membrane-bound GST fusion proteins, reacted with either an antibody specific to 55-kD E1B (2A6) [P. Sarnow, C. A. Sullivan, A. J. Levine, *Virology* **120**, 510 (1982)] or an E4orf6-specific antibody, RSA3 [M. J. Marton, S. B. Baim, D. A. Ornelles, T. Shenk, *J. Virol.* **64**, 2345 (1990)], and bound antibodies were detected with a horseradish peroxidase readout (ECL System, Amersham).
21. Human MCF7 cells were either mock-infected or infected with adenovirus at a multiplicity of 50 (*wt*300) or 250 plaque-forming units per cell (*dl*338 and *dl*355). Extracts were prepared 36 hours later and subjected to immunoprecipitation with the use of the p53-specific antibody DO-1. Immunoprecipitated proteins were analyzed by protein immunoblot assay with RSA3 antibody.
22. R. J. Grand, M. L. Grant, P. H. Gallimore, *Virology* **203**, 229 (1994).
23. Histidine-tagged E4orf6 purified from baculovirus-infected cells was tested for its ability to inhibit oligomerization of in vitro–translated p53 proteins [E. Shaulian, A. Zauberman, D. Ginsberg, M. Oren, *Mol. Cell. Biol.* **12**, 5581 (1992)] or to influence DNA binding in a band shift assay.
24. Histidine-tagged p53 (*13*) and E4orf6 proteins were purified from baculovirus-infected cells, and GST-$TAF_{II}31$ (*7*) was purified from *Escherichia coli*. Proteins captured by the GST-$TAF_{II}31$ fusion protein were analyzed by protein immunoblot assay with a mixture of antibodies to p53 (mAb 421) and E4orf6 (RSA3).

25. J. Milner and E. A. Medcalf, *Cell* **65**, 765 (1991).
26. T. D. Halazonetis, J. Davis, A. N. Kandil, *EMBO J.* **12**, 1021 (1993); T. D. Halazonetis and A. N. Kandil, *ibid.*, p. 5057; J. F. Waterman, J. L. Shenk, T. D. Halazonetis, *ibid.* **14**, 512 (1995).
27. L. E. Babiss and H. S. Ginsberg. *J. Virol.* **50**, 202 (1984); D. N. Halbert, J. R. Cutt, T. Shenk, *ibid.* **56**, 250 (1985); S. Pilder, M. Moore, J. Logan, T. Shenk, *Mol. Cell. Biol.* **6**, 470 (1986); D. H. Weinberg and G. Ketner, *J. Virol.* **57**, 833 (1986).
28. We thank N. Kley, H. Lu, J. Lin, and A. Levine for plasmids, A. Levine for critical reading of the manuscript, J. Cong for able technical assistance, and T.D. thanks H. Wolf for support in Regensberg. This work was supported by grants from NIH (T.S.) and the Infektionsforschung AIDS-Stipendienprogramm DKFZ (T.D.). S.R. received scholarship support from the University of Regensberg, and T.S. is an American Cancer Society Professor and an Investigator of the Howard Hughes Medical Institute.

5 January 1996; accepted 20 March 1996

Evidence That Spt6p Controls Chromatin Structure by a Direct Interaction with Histones

Alex Bortvin and Fred Winston*

Genetic analysis has implicated *SPT6*, an essential gene of *Saccharomyces cerevisiae*, in the control of chromatin structure. Mutations in *SPT6* and particular mutations in histone genes are able to overcome transcriptional defects in strains lacking the Snf/Swi protein complex. Here it is shown that an *spt6* mutation causes changes in chromatin structure in vivo. In addition, both in vivo and in vitro experiments provide evidence that Spt6p interacts directly with histones and primarily with histone H3. Consistent with these findings, Spt6p is capable of nucleosome assembly in vitro.

Chromatin structure plays an important role in the regulation of eukaryotic transcription (*1*). One subject of intensive study has been the Snf/Swi protein complex (*2*). Genetic, molecular (*3*), and biochemical analyses of the Snf/Swi complex from both yeast (*4*) and humans (*5*) have provided strong evidence that this complex helps transcription factors to bind to nucleosomal DNA. Genetic studies showed that particular histone mutations, such as a deletion of one of the two *H2A-H2B* gene pairs in the yeast genome (*hta1-htb1*)Δ, suppress *snf/swi* null mutations (*6*, *7*). The suppression of *snf2* and *snf5* mutations by this histone mutation occurs at the level of chromatin structure, as has been shown at *SUC2*, a Snf/Swi–dependent gene (*6*). In addition to mutations in histones, mutations in the nonhistone genes *SPT4*, *SPT5*, and *SPT6* also suppress *snf/swi* mutations (*3*). This and other common phenotypes suggest that the Spt4p, Spt5p, and Spt6p proteins are required for control of chromatin structure in yeast (*8*).

We analyzed the function of Spt6p, a large acidic nuclear protein that is essential for growth in *S. cerevisiae* (*9*). Mutations in *SPT6* restore the high levels of *SUC2* mRNA that are reduced by *snf/swi* mutations, thereby allowing growth on raffinose (*8*). The levels of suppression by *spt6* mutations are comparable to those achieved by the (*hta1-htb1*)Δ mutation (Fig. 1A) (*6*, *8*). However, mutations in *SPT6* have no significant effect on histone mRNA or protein levels (*10*).

Given the common phenotypes caused by (*hta1-htb1*)Δ and *spt6* mutations, we tested whether an *spt6* mutation also caused similar changes in chromatin structure. We therefore examined *SUC2* chromatin structure in *snf5* single mutants and *snf5 spt6* double mutants by indirect end-labeling of micrococcal nuclease (MNase)–digested chromatin (*11*). These results (Fig. 1B) demonstrate that in a *snf5* background, an *spt6* mutation causes the same changes in chromatin structure as does the (*hta1-htb1*)Δ histone mutation. In both *snf5 spt6* and *snf5* (*hta1-htb1*)Δ double mutants, cleavage by MNase around the TATA box and near the upstream activator sequence (UAS) was increased relative to the cleavage in a *snf5* single mutant (compare sites B, C, E, and F). These alterations in *SUC2* chromatin structure suggest that, in the *snf5* mutant, the presence of the nucleosomes over the promoter (*6*) is dependent on Spt6p. As shown previously for the suppression of *snf5* by (*hta1-htb1*)Δ, these *SPT6*-dependent changes in chromatin structure at the *SUC2* promoter are independent of the level of transcription because they occur at an enfeebled *SUC2* promoter that contains no TATA element (*10*). These results suggest that the primary effect of Spt6p in controlling transcription occurs by way of changes in chromatin structure.

Because *spt6* mutations cause changes in chromatin structure, it seemed possible that Spt6p might interact with histones. We reasoned that if the defect in *spt6* mutants is the result of a weakened interaction between Spt6p and histones, then an increased level of histones might restore the interaction. To overexpress histone genes,

Department of Genetics, Harvard Medical School, 200 Longwood Avenue, Boston, MA 02115, USA.

*To whom correspondence should be addressed.

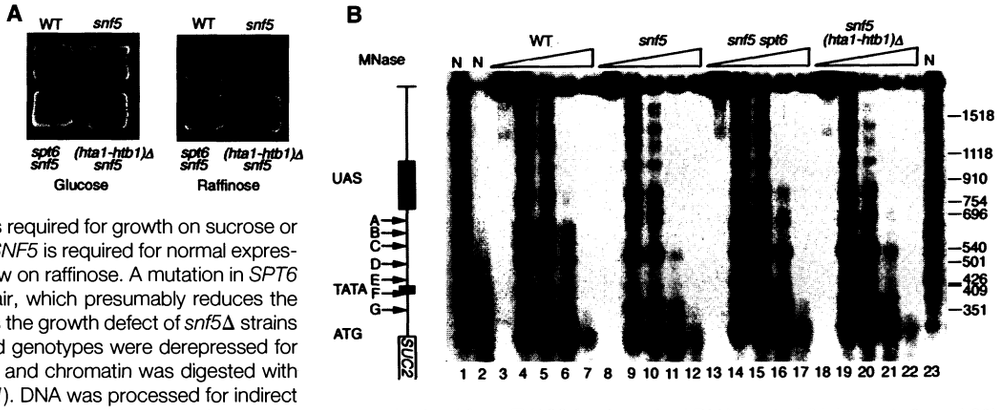

Fig. 1. An *spt6* mutation suppresses an *snf5* defect at the level of chromatin structure. (**A**) Patches of wild-type (WT) (FY120), *snf5*Δ (FY711), *spt6-140 snf5*Δ (ABY65), and (*hta1-htb1*)Δ *snf5*Δ (FY713) strains were grown on rich media and then replica-plated onto media containing either glucose or raffinose (*14*). The *SUC2* gene encodes invertase, which is required for growth on sucrose or raffinose as carbon sources. Because *SNF5* is required for normal expression of *SUC2*, *snf5*Δ mutants fail to grow on raffinose. A mutation in *SPT6* or deletion of the *HTA1-HTB1* gene pair, which presumably reduces the level of histones H2A and H2B, restores the growth defect of *snf5*Δ strains on raffinose. (**B**) Strains of the indicated genotypes were derepressed for *SUC2* expression, nuclei were purified, and chromatin was digested with increasing concentrations of MNase (*11*). DNA was processed for indirect end-labeling analysis of the *SUC2* promoter. Approximate positions of the *SUC2* promoter elements (UAS, the TATA element, and the translational start site) and MNase cleavage sites (arrows A through G) are indicated at left; positions of the size markers are shown at the right of the figure. DNA was obtained from FY120 for the naked DNA control (N, lanes 1, 2, and 23) and wild- type chromatin (lanes 3 through 7), from FY711 for *snf5* chromatin (lanes 8 through 12), from ABY65 for *snf5 spt6* chromatin (lanes 13 through 17), and from FY713 for (*hta1-htb1*)Δ *snf5* chromatin (lanes 18 through 22).